Title	Growth of p-type GaAsAlGaAs(111) quantum well infrared photodetector using solid source molecular-beam epitaxy
Author(s)	Li, H.; Mei, T.; Karunasiri, G.; Fan, Weijun; Zhang, Dao Hua; Yoon, Soon Fatt; Yuan, K. H.
Citation	Li, H., Mei, T., Karunasiri, G., Fan, W.., Zhang, D. H., Yoon, S. F., & Yuan, K. H. (2005). Growth of p-type GaAsAlGaAs(111) quantum well infrared photodetector using solid source molecular-beam epitaxy. Journal of applied physics, 98(5), 054905.
Date	2005
URL	http://hdl.handle.net/10220/18030
Rights	

Growth of *p*-type GaAs/AlGaAs(111) quantum well infrared photodetector using solid source molecular-beam epitaxy

H. Li and T. Mei[a)]
School of Electrical and Electronic Engineering, Nanyang Technological University, Singapore, 639798

G. Karunasiri
Department of Physics, Naval Postgraduate School, Monterey, California 93943

W. J. Fan, D. H. Zhang, S. F. Yoon, and K. H. Yuan
School of Electrical and Electronic Engineering, Nanyang Technological University, Singapore, 639798

(Received 29 November 2004; accepted 20 July 2005; published online 9 September 2005)

A *p*-type GaAs/AlGaAs multi-quantum-well infrared photodetector (QWIP) was fabricated on a GaAs (111)A substrate by molecular-beam epitaxy using silicon as dopant. The same structure was also grown on a GaAs (100) wafer simultaneously to compare the material and structural properties. It was found that Si acts as a *p*-type dopant in the GaAs (111)A sample while it is *n*-type in the GaAs (100) counterpart. The growth rate was found to be appreciably enhanced for GaAs (111)A compared with that of GaAs (100) orientation, while the Al composition in the barriers was found to be 20% smaller for a (111) orientation which results in a smaller barrier height. A peak responsivity of 1 mA/W with a relatively wide wavelength response ($\Delta\lambda/\lambda_p \sim 53\%$) was observed for the GaAs (111)A QWIP, mainly due to the location of the excited state far above the barrier. The photoresponse also showed a relatively strong normal incident absorption probably originating from the mixing of the conduction and valence Bloch states. The optimization of the quantum well parameters should further enhance the responsivity of this *p*-type QWIP with Si as dopant species. © *2005 American Institute of Physics*. [DOI: 10.1063/1.2034652]

I. INTRODUCTION

To date, most studies of III-V semiconductor quantum wells (QWs), superlattices, and heterostructures have utilized the conventional (100)-oriented substrates due to the relatively large window of good epitaxial growth conditions and the well-developed processing technology. Challenges exist in growing high quality material on non-(100) substrates. In contrast to two dangling bonds available for group-III surface adatoms in the (100) surface, three dangling bonds are available in the (111)A surface, which reduces the surface migration velocity of adatoms and increases the density of defects in the material.[1] However, due to the interest in investigating the effects of altering the fundamental material properties, growth mechanism, surface kinetics, and impurity incorporation, non-(100) plane substrates have also been utilized in previous studies.[2–5] An enhancement of optical transition in QWs grown on (111)B substrates and thus a reduced threshold current density of laser diode have been demonstrated.[6,7] Also, improved electron mobility in Si-doped (111)B AlGaAs has been observed.[8] Similar advantages have also been reported for heterostructures grown on (111)A substrates. The (111)-oriented *p*-type GaAs/AlGaAs quantum well infrared photodetector (QWIP) was theoretically investigated by Cho *et al.*,[9] and the absorption coefficient, responsivity, and detectivity were also estimated. *p*-type Si-doped AlGaAs/GaAs and AlGaAs/InGaAs QWIPs grown on (311)A substrates were reported and the dark current performance was compared with the Be-doped *p*-type QWIP grown on (100) substrate.[10]

In this paper, we report the preparation of a GaAs/AlGaAs QWIP structure on GaAs (111)A substrate grown by molecular-beam epitaxy (MBE) technology with Si as *p*-type dopant. The crystal and optical properties, doping behavior, and intersubband absorption are studied, and finally the QWIP detector is fabricated and characterized.

II. EXPERIMENTAL PROCEDURES

The GaAs/AlGaAs QWIP structure was grown on an undoped semi-insulating GaAs (111)A substrate by a solid source Riber 32 MBE system. The multi-quantum-well (MQW) structure consists of 30 periods of GaAs wells and AlGaAs barriers sandwiched by GaAs top and bottom contact layers. The growth structure along with the measured structural parameters is shown in Fig. 1. In addition, a GaAs

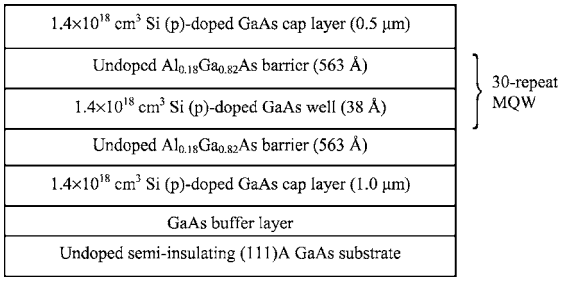

FIG. 1. The QWIP's growth structure with measured structural and composition parameters.

[a)]Electronic mail: ETMei@ntu.edu.sg

(100) substrate was also placed together with the (111)A substrate during the epitaxial growth to understand the effects of substrate orientation on growth parameters. Arsenic was supplied in the form of As_4 from a valved cracker cell and its beam equivalent pressure was fixed at 1.0×10^{-5} Torr during the growth. The substrates were outgassed in a preparation chamber before oxide desorption was performed by heating up the substrates to 590 °C with As_4 flux irradiation in the growth chamber. Silicon was incorporated as a *p*-type dopant in the (111)A-oriented QWIP sample. In order to maintain smooth morphology, the growth temperature was set at 650 °C and an As-rich growth condition (As_4/III flux ratio of ~23:1) was used. The Si cell temperature was fixed at 1020 °C during the growth of the GaAs wells and the contact layers. A 100-nm-thick GaAs buffer layer was grown before the growth of the QWIP structures.

After the growth, high-resolution x-ray diffraction (HRXRD) from the samples was measured using a Philips X'Pert material research diffractometer, which is equipped with a four-crystal Bartels monochromator in the high-resolution (220) scattering and a 0.65-mm slit in front of the detector to decrease the background intensity. The diffraction rocking curves were fitted by a computer program based on dynamical x-ray diffraction (XRD). In addition, the material quality of the QWIP structures was also characterized using low-temperature photoluminescence (PL). The electrochemical capacitance-voltage (*C-V*) profile was measured to determine the type and concentration of carriers. The infrared intersubband absorption of the samples was measured by a Fourier transform infrared (FTIR) spectrometer at room temperature with a 45°-polished multipass waveguide geometry. To facilitate the measurements of the *I-V* characteristics and responsivity, mesa diodes with an active area of about $200\times200\ \mu m^2$ were fabricated using standard photolithographic techniques and wet chemical etching. Au/Ti alloy was deposited using *e*-beam evaporation followed by lift-off and annealing in a rapid thermal processor at 410 °C to form *p*-type Ohmic contacts. A 45° facet was polished on the substrate for infrared light to illuminate the mesa diodes in experiments. The spectral dependence of the photoresponse was measured at low temperature using an Oriel 6575 infrared source coupled by an infrared lens to a Jobin Yvon Triax 320 monochromator. The photon flux of our system was measured using a calibrated Oriel 70124 pyroelectric detector. The photocurrent signal was amplified before inputing it into the lock-in amplifier. A ZnSe wire-grid polarizer placed after the monochromator allowed us to separate the contributions of 90°-polarized light (equivalent to normal-incident radiation or TE mode) and 0°-polarized light (TE and TM polarization modes in equal shares) from the responsivity spectra.

III. RESULTS AND DISCUSSION

Figure 2 shows the measured and simulated x-ray rocking curves of GaAs/AlGaAs QWIP structures grown on (111)A (sample A) and (100) (sample B) GaAs substrates. The zero-order satellite peaks (S_0) are clearly seen on the lower-angle side of the substrate peak. A set of higher-order

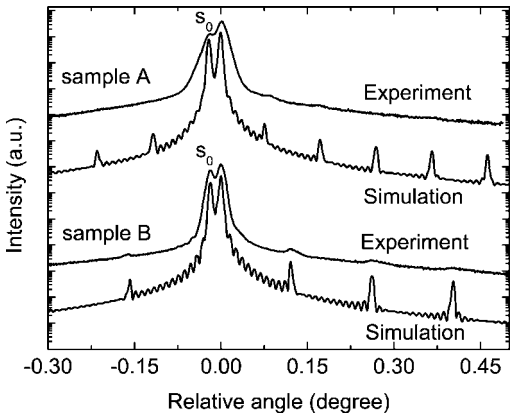

FIG. 2. Experimental x-ray rocking curves and simulated results for a 30-period GaAs/AlGaAs QWIP structure grown on (111)A (sample A) and (100) (sample B) substrates.

satellite peaks is discernible on the x-ray rocking curves for both samples but with diminutive intensities. This usually results from the small difference in lattice parameters between GaAs and AlGaAs layers and the small thickness of the GaAs well compared with the AlGaAs barrier. The average MQW periodicity can be derived from the angular spacing of the satellite peaks, and the simulated results are 601 Å (sample A) and 377 Å (sample B). Nearly a factor of two in the difference of the periodicity results from the dependence of MBE growth rate on substrate orientation. Under the same growth conditions, the average growth rates of AlGaAs and GaAs were calibrated to be about 1.18 and 0.88 μm/h on the (111)A substrate and 0.78 and 0.66 μm/h on the (100) substrate, respectively. Inherently, the epitaxial growth on the (111)A surface has a higher rate because there are three dangling bonds for each group-III adatom on the (111)A surface but only two on the (100) surface. Different from the growth rate on the (100) surface which is simply determined by Ga flux, the growth rate on the (111)A surface is associated with both the As_4/Ga flux ratio and the substrate temperature in a complex relation above 550 °C due to the limited dissociative chemisorption of As_4.[11]

Moreover, the Al compositions in AlGaAs epitaxial layers on (111)A and (100) surfaces are different in the calibration growth under the same growth conditions. This is also reflected in the angular position of S_0 in the x-ray rocking curve (see Fig. 2) which is related to the average composition for a GaAs/AlGaAs MQW structure.[12] The PL measurement data were incorporated to determine the well thickness and the Al fraction of AlGaAs barriers. As shown in Fig. 3, the PL spectra measured at 5 K for samples A and B have linewidths of approximately 13 and 6 meV, respectively. The transition between the ground electron and heavy-hole states (i.e., *E*1-*HH*1 transition) in (111)-oriented QWs is enhanced due to the larger heavy-hole mass along the (111) orientation,[7] which explains the observed higher PL intensity of sample A compared with sample B. The *E*1-*HH*1 transition energy as a function of barrier height and well width is obtained by estimating electron states using a transfer-matrix method within the effective-mass approximation, and *HH* states using a 4×4 Hamiltonian model[13] for the (111)A MQW and a 6×6 Hamiltonian model[14] for the (100) MQW.

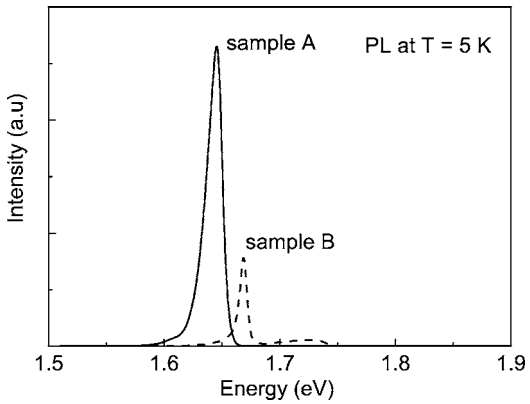

FIG. 3. PL spectra for samples A and B measured at 5 K.

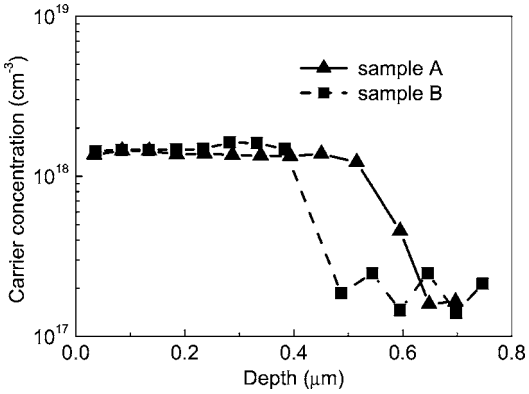

FIG. 4. Electrochemical *C-V* profiles of the Si-doped GaAs cap layers in samples A and B.

The parameters of band gap, effective mass, and band offset for (111)A- and (100)-oriented AlGaAs and GaAs epilayers were adopted from Refs. 13 and 15–17. The well thickness and the barrier composition were determined from the PL peak energy and the x-ray rocking curve simulation with several iterations until the calculation is in close agreement with experimental results. Using the above parameters, the calculated transition energies are 1.641 eV ($E1=86$ meV and $HH1=36$ meV) in comparison to the measured PL peak energy of 1.645 eV for the (111)A MQWs, and 1.672 eV ($E1=110$ meV and $HH1=43$ meV) in comparison to the measured PL peak energy of 1.669 eV for the (100) MQWs, respectively. The structural parameters listed in Table I confirm the reduction of a fraction of Al in the AlGaAs epitaxial layer on the (111)A surface, which is mainly due to the poor efficiency of Al atom adsorption to Ga atom site under a Ga-predominant (111)A surface. A similar phenomenon has been reported by Sanz-Hervás *et al.*[12] and Watanabe *et al.*[18] This makes the barrier height of the (111) QWIP much smaller than the (100) counterpart, pushing the excited state deep into the continuum.

The conduction type of incorporated Si atoms on the (111)A surface can be controlled by the growth conditions, such as the substrate temperature and V/III flux ratio.[19] Si atoms preferentially occupy Ga sites on a GaAs (100) surface that is terminated with double dangling bonds of both As and Ga atoms, and thus behave as donors under the arrival of excess As atoms. However, on a GaAs (111)A surface, each Ga atom has three bonds appending the surface while each As atom has only one. Therefore, Si atoms easily replace weakly bonded As atoms and behave as acceptors. The effect is enhanced at high growth temperature and low V/III flux ratio due to the reduction of As concentration on the surface. The doping concentrations and the conduction types were examined from the electrochemical *C-V* profiles of the Si-doped GaAs top contact layers of the two samples as shown in Fig. 4. A carrier concentration of about 1.4×10^{18} cm^{-3} is reached in both samples, but the dopants are *p*-type in sample A and *n*-type in sample B.

TABLE I. Experimental data and derived results from HRXRD measurement and PL spectra for samples A and B. L_w and L_b are the well and barrier widths, respectively, x is the aluminum fraction of the barrier, and E_p is the energy of the PL emission peak.

Samples	A: (111)A MQW	B: (100) MQW
x (%)	18	22
L_b (Å)	563	346
L_w (Å)	38	31
PL full width at half maximum (FWHM) (meV)	13	6
E_p (eV)	1.64	1.66

The dark current as a function of applied bias at different temperatures is given in Fig. 5 for the (111)A GaAs/AlGaAs QWIP. The symmetrical *I-V* characteristics are due to the symmetry between the GaAs growth on AlGaAs and the growth in reverse sequence, as well as negligible Si dopant migration along the growth direction, whereas Be doping always encounters fast outdiffusion.[10] Since the dark current at low bias and relatively high temperatures is dominated by thermionic emission,[20] it follows the $I(T)/T \propto \exp(-E_{ac}/k_BT)$ relationship. The activation energy E_{ac} can be extracted from the slope of the plot of the normalized dark current (I_d/T) versus the normalized inverse temperature $1000/T$ in semilog scale as shown in Fig. 6 for a set of bias voltages. The activation energies at different bias can be fitted quite well with the relation $E_{ac}=E_{ac0}\exp(-V/C)$ that is related to the reduction of barrier height due to the bias across the quantum well.[21] The extrapolated activation energy E_{ac0} at zero bias is approximately 59 meV and is in

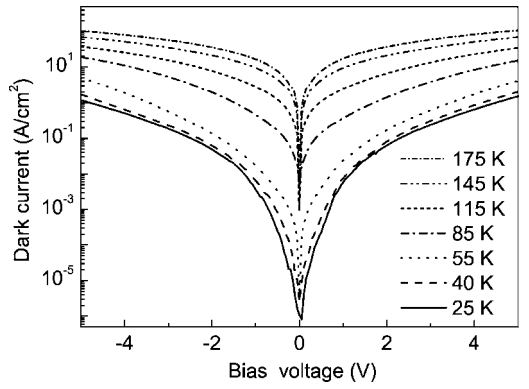

FIG. 5. *I-V* characteristics of the *p*-type (111)A GaAs/AlGaAs QWIPs under a series of temperatures.

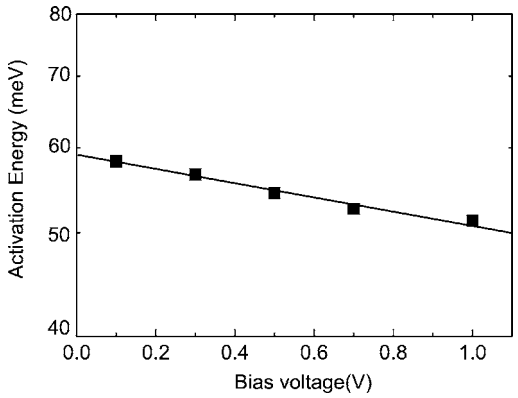

FIG. 6. The measured activation energy of the (111)A QWIP structure vs bias voltage.

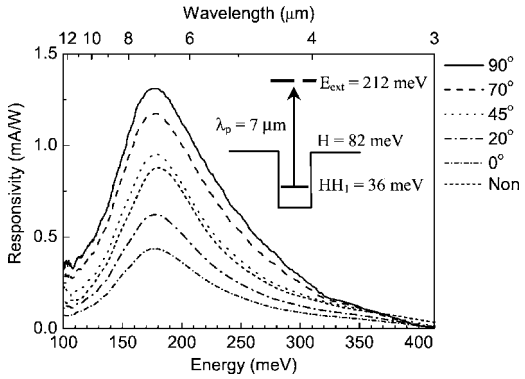

FIG. 8. The measured photocurrent spectra at 25 K and a bias voltage of 4.3 V. Infrared light is incident from a 45° facet polished on the substrate. 0° polarization refers to *p* polarization (TE+TM) and 90° polarization refers to *s* polarization (TE mode only). The nonpolarized spectra are also presented. The inset shows the energy-band diagram and the transition corresponding to the peak response.

agreement with the calculated value 61 meV using $E_{ac}=V_b+E_{ex}-HH1-E_F$, where V_b(=82 meV) and E_F(=2 meV) are the barrier energy height and the Fermi energy of a two-dimensional (2D) carrier gas referenced to the ground state, respectively. The E_{ex}(=17 meV) is the exchange energy due to the exchange effect in the quantum well.[22] The heavy-hole ground-state energy $HH1$ in *p*-type QWs and the electron ground-state energy E_1 in *n*-type QWs are derived using the QW structural parameters listed in Table I.

The normalized infrared-absorption spectra measured at room temperature and the photoresponse spectra measured at 25 K under bias voltage of 4.3 V are shown in Figs. 7 and 8, respectively. The photocurrent spectra are much wider ($\Delta\lambda/\lambda_p \sim 53\%$) than commonly reported results of (100) *p*-type GaAs/AlGaAs QWIPs (see Ref. 22, for example). This implies that the transitions occur from the ground state to continuum states far above the barrier. The energy levels of heavy-hole and light-hole states in (111)A-oriented GaAs/AlGaAs QWs are determined to be $HH1=36$ meV, $HH2=81$ meV, and $LH1=57$ meV, whereas the barrier height in the valence band is around 82 meV. Higher levels are in the continuum according to the calculation using the 4×4 effective-mass Hamiltonian model[13] for QWs grown on the (111) substrate. In our experiment, the photocurrent spectrum exhibits peak responsivity of about 1 mA/W, which is low compared with typical *p*-type QWIPs. The low peak responsivity is mainly due to the low doping concentration (equivalent 2D density, $N_D=5.7\times10^{11}$ cm^{-2}) and the large spectrum width $\Delta\lambda/\lambda_p$. This (111)A *p* QWIP has comparable peak responsivity to that of a low doping sample (sample A, $N_D=1\times10^{12}$ cm^{-2}) under the same bias in a study of doping density effects for (100) GaAs/AlGaAs *p* QWIPs,[23] whereas its photoresponse spectrum is much broader.

Normal incident response is usually expected in *p* QWIPs due to the interactions between components of *s*-symmetry states in the $LH(SO)$ subbands and *p*-symmetry states in the HH subbands.[24] However, in the present (111)A QWIP, we have observed the strongest response at normal incidence. Figure 9 shows that absorption and the photocurrent spectra of the *p*-type (111)A QWIP exhibit polarization dependence opposite to that in *n*-type QWIPs which observe the intersubband transition selection rule.[25,26] The peak responsivity is 1.3 mA/W for 90° polarization (*s* polarization, TE mode only), but only 0.4 mA/W for 0° polarization (*p* polarization, TE+TM modes). Therefore, the transition of in-plane (*x*-*y*) polarization is stronger than that of *z* polarization. In a *p*-type quantum well, transitions between heavy-hole states should be mainly sensitive to light polarized in the *z* direction, similar to the case of a *n*-type quantum

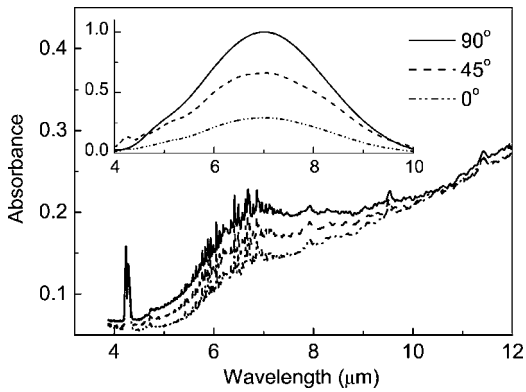

FIG. 7. Measured absorption spectra for the (111)A QWIP at 300 K using a waveguide structure. The inset shows the base line corrected data normalized to the maximum peak absorption.

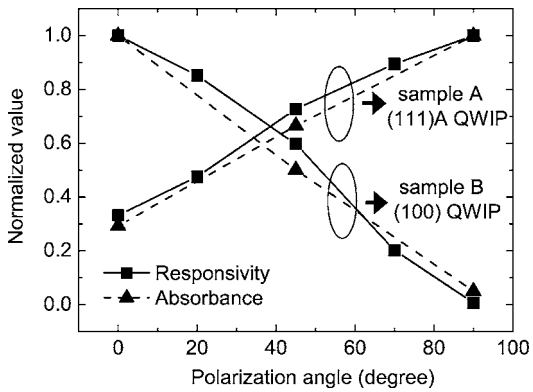

FIG. 9. Peak responsivity and peak absorption normalized to their respective maximum magnitudes vs the polarization angle for the *p*-type (111)A and the *n*-type (100) GaAs/AlGaAs QWIPs.

well.[27] Transitions of in-plane (x-y) polarization are expected to be strong between different hole bands (i.e., *HH* to *LH*).[24,28] For example, Szmulowicz and Brown,[28,29] Liu and co-workers[22,30] and Shen *et al.*[23] investigated a series of p-type GaAs/AlGaAs QWIPs and found the optimized p-type GaAs/AlGaAs QWIP for the strongest normal incident absorption has the final state for transition in resonance with the top of the barrier. By aligning *LH*2 in resonance with the top of the barrier in the (100) p QWIPs, Liu *et al.* obtained higher photoresponse of s polarization than p polarization.[30] However, in the (111)A QWIP, the peak normal incident response occurs when the final states are 130 meV above the top of the barrier. This indicates the highly mixed nature of the excited states far above the valence barrier and the interband processes that are allowed between p-symmetry and s-symmetry components.[24,31] The heavy hole has much larger effective mass along (111) than (100), while the light hole has slightly smaller effective mass along (111). This might also be a reason for the dominant normal incident response in the (111) p QWIP, since the lighter excited-state mass should give a better absorption and responsivity depending on the carrier transport.

IV. CONCLUSION

A p-type GaAs/AlGaAs QWIP structure on GaAs (111)A substrate was successfully grown with silicon as p-type dopant. The epitaxial growth rates of GaAs and AlGaAs were found to be enhanced while the Al incorporation was suppressed in the (111)A orientation compared to the (100) orientation. The positive carrier type was achieved using Si doping for the (111)A-oriented GaAs epitaxial layer, while the (100)-oriented GaAs layer showed n-type doping with nearly the same concentration. The (111)A GaAs/AlGaAs p QWIP gave the strongest photoresponse at normal incidence, indicating the strong mixing of conduction- and valence-band Bloch states. The measured valence-band offset of 82 meV amounts to about 36% of the total band offset between GaAs and $Al_{0.18}Ga_{0.82}As$ layers grown on (111)A substrate. The present QWIP sample has a responsivity of about 1 mA/W, but the responsivity can be further improved by optimizing the quantum well parameters and increasing the doping concentration to 10^{19} cm^{-3} which is the level typically used in p-type QWIPs.

ACKNOWLEDGMENTS

The authors would like to thank Tony Matos for critical reading of the manuscript.

[1] A. Chin and K. Chee, Appl. Phys. Lett. **68**, 3437 (1996).
[2] P. Ho, P. Martin, L. S. Yu, and S. S. Li, J. Vac. Sci. Technol. B **11**, 935 (1993).
[3] H. Q. Hou and C. W. Tu, J. Appl. Phys. **75**, 4673 (1994).
[4] H. Q. Hou, N. J. Sauer, and T. Y. Chang, 36th Electronic Materials Conference, Boulder, Colorado, 22–24 June 1994 (unpublished).
[5] A. Chin, P. Martin, P. Ho, J. Ballingal, T. Yu, and J. Mazurowski, Appl. Phys. Lett. **59**, 1899 (1991).
[6] T. Hayakawa, M. Kondo, T. Suyama, K. Takahashi, S. Yamamoto, and T. Hijikata, Jpn. J. Appl. Phys., Part 2 **26**, L302 (1987).
[7] T. Hayakawa, K. Takahashi, M. Kondo, T. Suyama, S. Yamamoto, and T. Hijikata, Phys. Rev. Lett. **60**, 349 (1988).
[8] A. Chin, T. M. Cheng, S. P. Peng, Z. Osman, U. Das, and C. Y. Chang, Appl. Phys. Lett. **63**, 2381 (1993).
[9] T. Cho, H. Kim, Y. Kwon, and S. Hong, Jpn. J. Appl. Phys., Part 1 **35**, 2164 (1996).
[10] A. Chin, C. C. Liao, J. Chu, and S. S. Li, J. Cryst. Growth **175/176**, 999 (1997).
[11] M. R. Fshy, K. Sato, and B. A. Joyce, Appl. Phys. Lett. **64**, 190 (1994).
[12] A. Sanz-Hervás, S. Cho, J. Kim, A. Majerfeld, C. Villar, and B. W. Kim, J. Cryst. Growth **195**, 558 (1998).
[13] J. B. Xia, Phys. Rev. B **43**, 9856 (1991).
[14] W. J. Fan, M. F. Li, T. C. Chong, and J. B. Xia, J. Appl. Phys. **80**, 3471 (1996).
[15] S. Cho, A. Sanz-Hervás, and A. Majerfeld, Phys. Rev. B **68**, 035308 (2003).
[16] S. L. Chuang, *Physics of Optoelectronic Devices* (Wiley, New York, 1995), p. 710.
[17] J. Los, A. Fasolino, and A. Catellani, Phys. Rev. B **53**, 4630 (1996).
[18] T. Watanabe, T. Yamamoto, P. O. Vaccaro, H. Ohnish, and K. Fujita, Microelectron. J. **27**, 411 (1996).
[19] K. Sato, M. R. Fshy, M. L. Ashwin, and B. A. Joyce, J. Cryst. Growth **165**, 345 (1996).
[20] S. Y. Wang and C. P. Lee, J. Appl. Phys. **82**, 2680 (1995).
[21] D. H. Zhang and W. Shi, Appl. Phys. Lett. **73**, 1095 (1998).
[22] H. C. Liu, L. Li, M. Buchanan, Z. R. Wasilewski, G. J. Brown, F. Szmulowicz, and S. M. Hegde, J. Appl. Phys. **83**, 585 (1998).
[23] A. Shen, H. C. Liu, F. Szmulowicz, M. Buchanan, M. Gao, G. J. Brown, and J. Ehret, J. Appl. Phys. **86**, 5232 (1999).
[24] P. Man and D. S. Pan, Appl. Phys. Lett. **61**, 2799 (1992).
[25] D. D. Coon and R. P. G. Karunasiri, Appl. Phys. Lett. **45**, 649 (1984).
[26] L. C. West and S. J. Eglash, Appl. Phys. Lett. **46**, 1156 (1985).
[27] H. C. Liu, M. Buchanan, and Z. R. Wasilewski, Appl. Phys. Lett. **72**, 1682 (1998).
[28] F. Szmulowicz and G. J. Brown, Phys. Rev. B **51**, 13203 (1995).
[29] F. Szmulowicz and G. J. Brown, Appl. Phys. Lett. **66**, 1659 (1995).
[30] H. C. Liu, F. Szmulowicz, Z. R. Wasilewski, M. Buchanan, and G. J. Brown, J. Appl. Phys. **85**, 2972 (1999).
[31] A. Fenigstein, E. Finkman, G. Bahir, and S. E. Schacham, J. Appl. Phys. **76**, 1998 (1994).